

The Stability of Intermediate Chlorites of the Clinocllore-Daphnite Series at 2 Kbar P_{H_2O}

A. W. McONIE, J. JEFFREY FAWCETT, AND R. S. JAMES¹

Department of Geology, University of Toronto,
Toronto, Canada M5S1A1

Abstract

The upper stability limits for intermediate magnesium-iron chlorites of the clinocllore-daphnite solid solution series were investigated at 2.07 kbar water pressure equal to total pressure at oxygen fugacities defined by the nickel-nickel oxide buffer. Five distinct high temperature breakdown assemblages of chlorite have been found: (i) cordierite₈₈ + olivine₈₈ + spinel₈₈ from Chl₁₀₀Da₀ to Chl₆₅Da₃₅, (ii) cordierite₈₈ + olivine₈₈ + hercynite₈₈ from Chl₆₅Da₃₅ to Chl₄₇Da₅₃, (iii) cordierite₈₈ + olivine₈₈ + magnetite₈₈ from approximately Chl₄₇Da₅₃ to Chl₄₅Da₅₅, (iv) cordierite₈₈ + orthoamphibole₈₈ + magnetite₈₈ from Chl₄₅Da₅₅ to Chl₂₇Da₇₃, and (v) cordierite₈₈ + quartz + magnetite₈₈ from Chl₂₇Da₇₃ to Chl₀Da₁₀₀. The upper limit of chlorite stability varies over the temperature range 720° to 535°C between the clinocllore and daphnite end members respectively.

Unit cell parameters for synthetic chlorites of the clinocllore-daphnite solid solution series have been computed and expressed as functions of composition. Electron microprobe analyses of synthetic cordierite indicate a relatively uniform variation in composition with up to 11.9 wt percent iron as FeO in solid solution. The composition of the orthoamphibole phase has been calculated to be intermediate between anthophyllite and gedrite, with a small amount of iron substitution.

The results are applicable in the interpretation of some contact metamorphic assemblages derived from ultramafic rocks, and are used to explain the origin of cordierite-anthophyllite bearing rocks found in chlorite alteration pipes below the base metal deposits of the Noranda area.

Introduction

An understanding of the phase equilibria in the system MgO-FeO-Al₂O₃-SiO₂-H₂O is necessary to understand the mineral assemblages of metamorphic rocks whose chemical compositions lie close to this system. The present study was concerned with the upper stability limits for intermediate magnesian-iron chlorites of the clinocllore-daphnite solid solution series at a total water pressure of 30,000 p.s.i. (2.07 kbar) with the oxygen fugacity defined by the nickel-nickel oxide buffer. Results of the present study combined with the results of other low-pressure phase equilibria studies in this system are applicable in the interpretation of the mineral assemblages of ultramafic rocks that have been re-equilibrated in contact metamorphic environments.

A substantial amount of experimental work has

been done on the synthesis and stability of magnesian and ferrous end members of the chlorite series (Yoder, 1952; Nelson and Roy, 1958; Turnock, 1960; Segnit, 1963; Fawcett and Yoder, 1966; Chernosky, 1974; James, Turnock, and Fawcett, 1974, unpublished). Unfortunately, some of the reported reactions have not been reversed and the reaction products have sometimes been shown to be metastable assemblages. Fawcett and Yoder (1966) determined the upper stability limits of clinocllore up to 10 kilobars water pressure with the breakdown curve passing through the points 768 ± 7°C at 3.5 kbar, 787 ± 7°C at 5 kbar and 830 ± 5°C at 10 kbar. Two stable breakdown assemblages were established: enstatite + forsterite + spinel + vapor above 3.5 kbar; and cordierite + forsterite ± spinel + vapor at lower pressure. Zen's (1972) discussion of the thermodynamic properties of minerals points out the limitations of reversal data in that study. James *et al* (1974) determined the upper stability of the iron chlorite daphnite up to 8 kilobars water pressure with

¹ Now at Department of Geology, Laurentian University, Sudbury, Ontario.

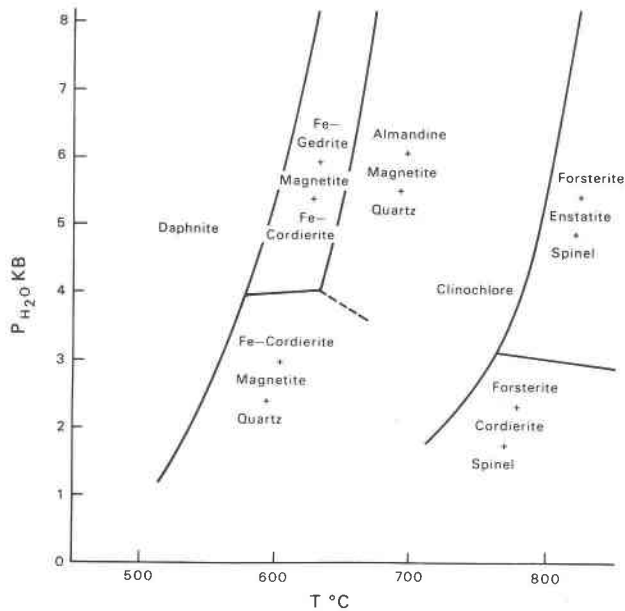


FIG. 1. Upper stability limits of clinocllore (Fawcett and Yoder, 1966) and daphnite (James *et al.*, 1974), the latter at the NNO buffer.

the partial pressure of oxygen defined by the nickel-nickel oxide buffer. The following points on the breakdown curve were defined by reversed reactions: 537°C and 2 kbar, 575°C and 4 kbar, 604°C and 6 kbar and 627°C and 8 kbar. Two high temperature breakdown assemblages were defined: iron cordierite + magnetite + quartz + vapor, below 4 kbar water pressure; and iron gedrite + magnetite + cordierite + vapor at higher pressures. Figure 1 illustrates the important features of the studies discussed above.

Hydrothermal Experiments

Standard hydrothermal techniques and laboratory equipment were used during this study. For water pressures of 30,000 p.s.i. (2.07 kilobars) standard rod-bombs made of Rene 41 alloy, with a conven-

TABLE 1. Mineral Abbreviations and Compositions

Chlorite solid solution	Chl	$5(\text{Mg}, \text{Fe})\text{O} \cdot \text{Al}_2\text{O}_3 \cdot 3\text{SiO}_2 \cdot 4\text{H}_2\text{O}$
Clinocllore-Daphnite solid solution	Chl-Da	$5(\text{Mg}, \text{Fe})\text{O} \cdot \text{Al}_2\text{O}_3 \cdot 3\text{SiO}_2 \cdot 4\text{H}_2\text{O}$
Cordierite solid solution	Co	$2(\text{Mg}, \text{Fe})\text{O} \cdot 2\text{Al}_2\text{O}_3 \cdot 5\text{SiO}_2$
Enstatite	En	$\text{MgO} \cdot \text{SiO}_2$
Hercynite-Spinel solid solution	Hc-sp	$(\text{Mg}, \text{Fe})\text{O} \cdot \text{Al}_2\text{O}_3$
Magnetite rich solid solution	Mt	$\text{FeO} \cdot (\text{Fe}^{3+}, \text{Al})_2\text{O}_3$
Olivine solid solution	Ol	$2(\text{Mg}, \text{Fe})\text{O} \cdot \text{SiO}_2$
Orthorhombic amphibole solid solution	Ged	$6(\text{Mg}, \text{Fe})\text{O} \cdot 1\frac{1}{2}\text{Al}_2\text{O}_3 \cdot 6\text{SiO}_2 \cdot \text{H}_2\text{O}$
Quartz	Qtz	SiO_2
Talc solid solution	Tc	$6(\text{Mg}, \text{Fe})\text{O} \cdot 0.8\text{SiO}_2 \cdot 4\text{H}_2\text{O}$

tional cone-in cone seal (Tuttle, 1949) were employed. The pressure vessels were heated in vertical Hevi-Duty Co. nichrome or chromel-C alloy resistance furnaces. Each furnace was controlled by either a Barber-Coleman Co. on-off controller (model 471) or by a Thermo-Electric Co. proportional controller (model 32422).

The experimental method used for buffering the oxygen fugacity within the pressure vessels was that developed by Eugster (1957, 1959). Nickel-nickel oxide buffers were made from Fisher reagent grade chemicals mixed in equal proportions, and after being used in an experiment the buffer was checked by X-ray diffraction for the presence of both phases.

The charges were either a mixture of MgO, FeO, Al_2O_3 , and SiO_2 in the stoichiometric proportions of the compositions investigated or the crystalline products of prior experiments. The following reagents were used in the preparation of the oxide mixtures: *ferrous oxalate*—British Drug House (lot 2859800) heated in air or in hydrogen to produce metallic iron or Fe_2O_3 ; *aluminum hydroxide*—Fisher Certified Reagent (lot 764180) heated in air to produce $\lambda \text{Al}_2\text{O}_3$; *magnesium carbonate*—Fisher Certified Reagent (lot 762372) heated in air to produce MgO; *silica*—Fisher Certified Reagent (lot 753025).

The technique used for reversing reactions was the re-running of equilibrium assemblages of synthetic phases under different physical conditions. The run products were examined as a function of time and the direction of the reaction was determined by noting changes in relative abundances of the participating phases as indicated by X-ray diffraction and optical examination. Most bulk compositions investigated lie on the clinocllore and daphnite join (with the exception of daphnite₉₀ clinocllore₁₀) and are indicated on Figure 7. Table 1 lists the mineral phases that were encountered, and Figure 2 indicates the extent of solid solutions involved in these species.

Description of the Mineral Phases

Methods of Identification

Because of the extremely small grain size of most of the run products, identification was based exclusively on X-ray diffraction methods. The measurement of refractive indices was not always possible due to the extremely small grain size of most of the mineral phases. However, some measurements were made, using white light at room temperature.

Detailed X-ray examination was carried out with a large diameter ($r = 57.3$ mm) Debye-Scherrer powder

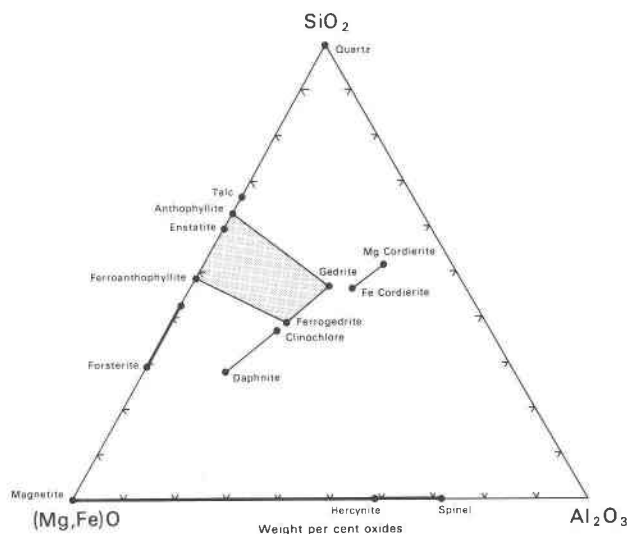


FIG. 2. Phases encountered in the experiment products.

camera using the Straumanis arrangement. Exposure times between 10 and 24 hours were used for either Ni filtered $CuK\alpha$ radiation or Mn filtered $FeK\alpha$ radiation.

An internal quartz standard was used with chlorite samples, and sufficient back reflections were present from the breakdown assemblages to make these films self-calibrating. Powder camera films sometimes revealed the presence of very small quantities of phases not detected by the diffractometer. Cell parameters were computed using a least squares refinement program written by Appleman, Handwerker, and Evans (1963). Quantitative electron microprobe analyses were possible on some of the larger grains of cordierite.

Chlorite $(Mg,Fe)_5Al_2Si_3O_{18}(OH)_8$

Chlorite characteristically occurred as aggregates of extremely thin hexagonal plates that were, on the average, approximately 0.01 mm across. The grains showed very low birefringence and were not normally hosts to inclusions. Mean refractive index determinations were made in white light for chlorites of most compositions; these are shown in Figure 3 and listed on Table 2. These closely follow the relation derived by Hey (1954) from the data of natural chlorites.

Hey demonstrated that the a and b cell parameters of natural chlorites increase with increasing substitution of Fe or Mn for Mg and that they are relatively uninfluenced by Al content. He noted that d_{001} was independent of Fe^{2+} but that it decreased slightly with an increase of Fe^{3+} . He found this basal spacing to be influenced principally by the substitution of Al for Si.

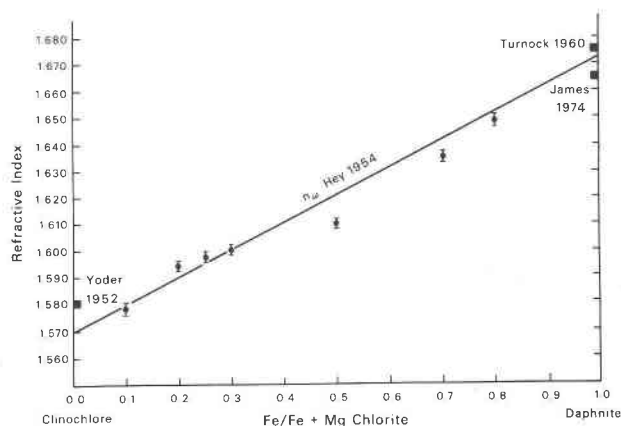


FIG. 3. Mean refractive indices of synthetic chlorites. The line derived by Hey (1954) was based on indices of natural chlorites. See Table 2.

Unit cell parameters for synthetic chlorites of the clinocllore-daphnite series were determined on the basis of the monoclinic space group $C2/m$. During the refinements the input parameters were not the same in each case but were close to $a_0 = 5.35$, $b_0 = 9.3$, and $c_0 = 14.25(\text{\AA})$. Those used in the final refinement were selected to be those which gave the smallest deviations and the greatest degrees of freedom. All reflections were measured relative to an internal quartz standard; the data are presented in Table 3. The results of the unit cell refinements (Table 4, Fig.

TABLE 2. Mean Refractive Index of Synthetic Chlorites of the Clinocllore-Daphnite Solid Solution Series

Composition	Sample number	n calc. (1)	n_{mean}
$Chl_{100}Da_0$	(2)	1.570	1.580
$Chl_{100}Da_0$	(3)	1.570	1.572
$Chl_{90}Da_{10}$	146(C)F	1.580	1.578±0.002
$Chl_{80}Da_{20}$	141F	1.590	1.594±0.002
$Chl_{75}Da_{25}$	25F	1.595	1.597±0.002
$Chl_{70}Da_{30}$	157M	1.600	1.600±0.002
$Chl_{60}Da_{40}$		1.610	n.d.
$Chl_{50}Da_{50}$	156M	1.621	1.610±0.002
$Chl_{40}Da_{60}$		1.632	n.d.
$Chl_{30}Da_{70}$	180(A)M	1.643	1.635±0.002
$Chl_{25}Da_{75}$		1.648	n.d.
$Chl_{20}Da_{80}$	182M	1.653	1.650±0.002
$Chl_{10}Da_{90}$		1.663	n.d.
Chl_0Da_{100}	(4)	1.673	1.675±0.006
Chl_0Da_{100}	(5)	1.673	1.665±0.005

(1) Hey, 1954
 (2) Yoder, 1952
 (3) Clinocllore (Deer, Howie and Zussman, vol. 3, anal. 24, p. 142)

(4) Turnock, 1960
 (5) James *et al.*, 1974

TABLE 3. Observed *d* Spacings for Synthetic Chlorites⁽¹⁾

Bulk Compn.	Chl ₁₀₀ Da ₀	Chl ₉₀ Da ₁₀	Chl ₈₀ Da ₂₀	Chl ₇₅ Da ₂₅	Chl ₇₀ Da ₃₀	Chl ₆₀ Da ₄₀	Chl ₅₀ Da ₅₀	Chl ₃₀ Da ₇₀	Chl ₂₅ Da ₇₅	Chl ₂₀ Da ₈₀	Chl ₀ Da ₁₀₀	I/I ₀
Run No.	294F (2)	146(C) F	141F	17F	157M	136F	156M	180(A)M	178(A)M	182M	226J (3)	
hkl	d obs (Å)	I/I ₀										
001	n.d.	14.333	14.273	14.169	14.232	14.296	14.260	14.205	14.324	14.168	14.137	9
002	7.140	7.114	7.147	7.124	7.133	7.079	7.124	7.074	7.076	7.097	7.079	10
003	4.760	4.746	4.764	4.752	4.754	4.735	4.743	4.715	4.724		4.698	4
020												
110	4.590	4.574	4.581	4.599	4.609	4.581	4.617			4.638		2
021				4.379				4.388		4.409		1
112							4.076					1
022								3.893				1
112			3.705	3.686	3.673	3.684	3.679	3.662	3.686	3.662		2
004	3.570	3.557	3.566	3.554	3.559	3.599	3.543	3.538	3.548	3.538	3.522	10
113	3.130		3.125	3.124			3.124					2
114				2.965			2.958					2
005	2.850	2.856	2.835	2.847	2.857	2.855	2.843	2.826	2.819	2.965	2.817	4
024					2.803	2.795						1
131				2.661							2.680	1
130	2.640											
131				2.587	2.602	2.597	2.600	2.609	2.603		2.617	3
202	2.580	2.583										
201			2.549	2.553	2.550	2.556	2.564	2.564	2.564		2.572	4
135	2.540	2.539										
115						2.521	2.529	2.521				1
203												
132	2.440	2.441									2.463	3
025								2.413				1
133			2.383	2.387	2.396	2.391	2.382	2.396	2.398	2.395	2.406	3
202	2.380											
006		2.356					2.361		2.354			1
220												
133						2.236						1
221												
116								2.193				1
026				2.099				2.103				1
043												
205	2.070		2.078			2.079			2.091	2.094		2
134												
224	2.030	2.043		2.039			2.045		2.040			1
116												
204	2.000	1.999	2.008	2.010	2.009		2.011	2.017	2.011		2.013	5
135												
225	1.886	1.883	1.887	1.892	1.888	1.885	1.886	1.890			1.888	3
206												
205	1.828					1.830						2
045	1.787											1
117								1.777				1
008												1
151	1.735					1.767						1
151	1.717											1
152				1.711								1
136										1.709		1
311												
152							1.686					1
243												
137	1.667		1.663	1.666		1.668	1.664	1.659	1.669			2
206												
243											1.607	1
315					1.567	1.572		1.570				3
009												4
208	1.570	1.569	1.570									4
060	1.535	1.537		1.541	1.542	1.544	1.543	1.554	1.553	1.559	1.564	6
119								1.543	1.540	1.542		1
047		1.521										1
331	1.499	1.501	1.503	1.505	1.508	1.509			1.517	1.520		4
062												
314				1.483								1
0,0,10	1.424											1
315												1
139			1.400									1
2,0,10			1.323									1
0,0,11			1.292									1

(1) All *d* obs. are accurate to $\pm 0.1^\circ 2\theta$ for Fe K α radiation

(2) Chlorite of clinoclone composition crystallised at 690°C and 30,000 p.s.i.

(3) Chlorite of daphnite composition crystallised at 595°C and 72,000 p.s.i.

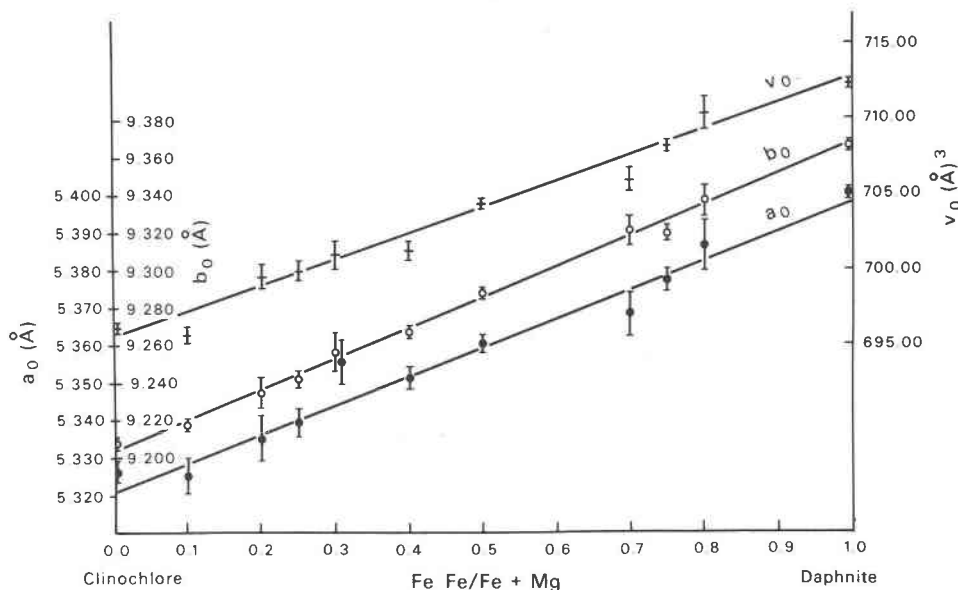


FIG. 4. Cell dimensions of synthetic chlorites on the clinocllore-daphnite join (see Table 4). Straight lines were obtained from linear regression equations—see text for correlation coefficients.

4) indicate a strong linear relation of the a_0 and b_0 cell parameters to the chlorite composition. Linear regression equations have been calculated to show the following relations where X is $Fe/(Fe + Mg)$ of the chlorite and r is the correlation coefficient:

$$a_0 = 5.3224 + 0.0751X \quad r = 0.982$$

$$b_0 = 9.2039 + 0.1619X \quad r = 0.998$$

$$c_0 = 14.309 - 0.103X \quad r = 0.874$$

$$v_0 = 695.40 + 17.03X \quad r = 0.986$$

These values compare favorably with those calculated from Hey's equations, although b_0 is slightly larger than expected. It can be seen that the value of d_{001} is not constant for these chlorites of fixed Al content. However, the slight decrease of c_0 with total iron content may be correlated with the increase in the amount of Fe^{3+} present. There is no consistent relation between d_{001} and Mg-Fe ratio but the data tend to support Bailey's (1972) observation that synthetic chlorites generally have larger d_{001} values than natural chlorites of similar composition.

Olivine $(MgFe)_2SiO_4$

Olivine occurred as small (maximum size 0.05 × 0.01 mm) pale green euhedral grains. The refractive indices n_α and n_β were determined, where possible, for olivine coexisting with cordierite and spinel (Table 5).

Unit cell parameters computed on the basis of an orthorhombic cell (space group $Pbnm$) with $a_0 = 4.8$,

$b_0 = 10.2$, and $c_0 = 6.0$ (Å) show a clear linear relationship with the composition of the olivine as listed in Table 6. Olivine compositions were estimated by the d_{130} diffraction method using the equation determined for synthetic olivines by Fisher (1966).

Cordierite $Al_3(Mg,Fe)_2AlSi_5O_{18}$

Cordierite occurred as colorless lath-shaped grains up to a maximum size of 0.25 mm across. The refractive indices for n_α and n_β shown in Table 7 indicate a pronounced increase with the iron content of the bulk composition from which they were synthesized. These closely follow the trend indicated by Hsu and Burnham (1969) for synthetic end-member cordierites grown at 2 kilobars water pressure.

Unit cell parameters of cordierite coexisting with olivine and hercynite-spinel, computed on the basis of the orthorhombic space group $Cccm$ for a cell with $a_0 = 9.7$, $b_0 = 17.1$, and $c_0 = 9.4$ (Å), show a distinct increase of V_0 with iron content of the bulk composition of the starting material (Table 8).

Several cordierite grains, chosen for their apparent optical homogeneity and lack of inclusions, were analyzed simultaneously for Si, Mg and Fe at a large number of spots within the grain using an electron microprobe (Table 9). The compositions were computed using a revised form of Rucklidge's data reduction program (Rucklidge, 1969; Rucklidge *et al.*, 1970) on the basis of a fixed stoichiometry with Al =

TABLE 4. Cell Parameters of Synthetic Chlorites

Composition	Run No.	$a_0(\text{\AA})$	$b_0(\text{\AA})$	$c_0(\text{\AA})$	$v_0(\text{\AA})^3$	N
Chl ₁₀₀ Da ₀	294F (1)	5.326 ± 0.003	9.208 ± 0.003	14.307 ± 0.013	696.06 ± 0.48	20
Chl ₉₀ Da ₁₀	146(C)F	5.325 ± 0.005	9.217 ± 0.004	14.287 ± 0.001	695.66 ± 0.68	19
Chl ₈₀ Da ₂₀	141F	5.335 ± 0.006	9.234 ± 0.009	14.320 ± 0.000	699.58 ± 0.91	26
Chl ₇₅ Da ₂₅	17F	5.339 ± 0.004	9.241 ± 0.005	14.304 ± 0.011	699.81 ± 0.62	28
Chl ₇₀ Da ₃₀	157M	5.355 ± 0.006	9.256 ± 0.011	14.251 ± 0.016	701.07 ± 1.08	20
Chl ₆₀ Da ₄₀	136F	5.351 ± 0.003	9.267 ± 0.004	14.251 ± 0.10	701.25 ± 0.60	15
Chl ₅₀ Da ₅₀	156M	5.360 ± 0.002	9.287 ± 0.002	14.265 ± 0.005	704.47 ± 0.32	15
Chl ₃₀ Da ₇₀	180(A)M	5.368 ± 0.006	9.321 ± 0.008	14.221 ± 0.008	705.96 ± 0.86	19
Chl ₂₅ Da ₇₅	178(A)M	5.377 ± 0.003	9.319 ± 0.003	14.244 ± 0.006	708.06 ± 0.44	18
Chl ₂₀ Da ₈₀	182M	5.386 ± 0.009	9.337 ± 0.008	14.244 ± 0.019	710.39 ± 1.17	12
Chl ₀ Da ₁₀₀	226J (2)	5.400 ± 0.001	9.365 ± 0.002	14.198 ± 0.003	712.29 ± 0.21	17

(1) Chlorite of clinocllore composition crystallized at 690°C and 30,000 p.s.i.

(2) Chlorite of daphnite composition crystallized at 595°C and 72,000 p.s.i.

2.0(Mg + Fe). Thus, the analyses that were affected by contamination by inclusions of phases other than cordierite gave totals that do not closely approximate the ideal 100 percent. Figure 5 illustrates the relatively large range of composition found within each sample. Some of this variation may be accounted for by contamination by inclusions. It seems likely, however, that a true homogeneous equilibrium was not attained in every case. The magnesium-rich cordierites appear to be slightly silica deficient, or slightly alumina enriched, compared with the ideal cordierite composition. This may be correlated with the decrease in total iron content or in Fe³⁺. There is no apparent discontinuity in the composition of cordierite at the reaction boundary separating the olivine and orthoamphibole fields (see experimental results below).

Orthoamphibole (Mg,Fe)₈₋₅Al₁₋₂Si₆(Al,Si)₂O₂₂(OH)₂

Orthorhombic amphibole occurred as tiny length-slow needles with an average grain size less than 0.005 mm in length. This extremely small grain

TABLE 5. Refractive Index Determinations of Olivine Coexisting with Cordierite and Spinel

Bulk Composition	Sample No.	$n_{\alpha'}$	n_{β}	% Fo
Chl ₉₀ Da ₁₀	161M	1.640 ± 0.001	1.670 ± 0.001	Fo ₉₄
Chl ₇₅ Da ₂₅	163M	1.660 ± 0.002	n.d.	Fo ₈₆
Chl ₅₀ Da ₅₀	173M	1.717 ± 0.002	1.728 ± 0.002	Fo ₅₅

Olivine compositions are based on the curves of Deer, Howie and Zussman (1962), p. 22.

size precluded any refractive index determinations. It was possible to estimate the amphibole composition in one assemblage of cordierite + magnetite₈₈ + amphibole after analyzing cordierite with the electron probe and estimating the magnetite composition from X-ray data. The calculation was based on a knowledge of the bulk composition of the experimental charge and on the erroneous assumption that all iron was present as FeO. The oversimplified calculation suggested that the amphibole was an intermediate aluminous variety in the anthophyllite-gedrite solid solution series. X-ray data for four samples is presented in Table 10 and calculated amphibole compositions in Table 11.

Spinel (Mg,Fe)Al₂O₄-Fe₃O₄

The oxide phases were always extremely fine grained, with the average grain size being less than 0.005 mm. These minerals characteristically occurred as euhedral crystals with a cubic habit. No satisfactory refractive index determinations were made. X-ray data for nine samples are shown in Table 12.

The results of calculations of unit cell sizes (Table 12) show that three distinct groups of oxide phases were encountered as illustrated in Figure 6. Magnetite and spinel show a linear increase in a_0 with bulk composition. No X-ray determinative methods are available for the compositions of phases in the MgAl₂O₄-FeAl₂O₄ solid solution series, and the compositions given in Table 12 were estimated by assuming that a linear increase in a_0 between the spinel and hercynite end members was related to composition. All other compositions were estimated using the rela-

TABLE 6. Cell Parameters and Compositions of Synthetic Olivine Coexisting with Cordierite and Hercynite-Spinel

	Forsterite	Chl ₉₀ Da ₁₀	Chl ₈₀ Da ₂₀	Chl ₇₀ Da ₃₀	Chl ₆₀ Da ₄₀	Chl ₅₀ Da ₅₀
Run No.	(1)	160M	148(C)F	147	142	173M
a_o (Å)	4.756	4.755 ± 0.001	4.769 ± 0.002	4.768 ± 0.002	4.783 ± 0.002	4.778 ± 0.002
b_o (Å)	10.195	10.221 ± 0.005	10.259 ± 0.007	10.288 ± 0.005	10.297 ± 0.008	10.312 ± 0.008
c_o (Å)	5.981	5.991 ± 0.003	6.002 ± 0.004	6.008 ± 0.003	6.017 ± 0.003	6.028 ± 0.004
V_o (Å) ³	290.00	291.15 ± 0.15	293.62 ± 0.24	294.69 ± 0.19	296.30 ± 0.23	296.99 ± 0.25
d_{130} (Å)		2.7704 ± 0.0030	2.7793 ± 0.0030	2.7845 ± 0.0030	2.7907 ± 0.0030	2.7903 ± 0.0030
% Fo (2)		Fo ₉₅	Fo ₈₀	Fo ₇₃	Fo ₆₄	Fo ₆₀

(1) from Yoder and Sahama (1957).

(2) from Fisher (1966).

tion derived by Turnock and Eugster (1958). In every case only one oxide phase was found to be present in the stable assemblages.

The temperatures for the formation of the synthesized spinel phases lie below the upper limit of the solvus defined for the hercynite-magnetite series by Turnock and Eugster (1962). It might be expected, therefore, that some assemblages would contain two coexisting spinel phases. This was not observed, and it is considered that the distinct breaks between the three groups of spinels represent reaction boundaries rather than subsolvus relations.

Quartz SiO_2

Quartz commonly occurred in the iron-rich portion of the phase diagram and was usually one of the first minerals to crystallize regardless of temperature. It persisted for great lengths of time as a reaction product but was normally shown to be metastable.

Unstable Phases

The unstable phases encountered were the 7Å chlorite polymorph, talc, enstatite, and an unidentified 10Å phase.

Experimental Results

Five assemblages have been defined as the high temperature breakdown products of chlorites of the clinocllore-daphnite solid solution series at a total water pressure of 30,000 p.s.i. (2.07 kbar) and at oxygen fugacities defined by the nickel-nickel oxide buffer; these are shown in Figure 7.

The upper stability of the clinocllore and daphnite end members have been taken from Fawcett and Yoder (1966) and James *et al* (1974) respectively. The

breakdown assemblages along the equilibrium curve are as follows:

- (1) cordierite₈₈ + olivine₈₈ + spinel₈₈ from Chl₁₀₀Da₀ to Chl₆₅Da₃₅ over the temperature range 720–680° (± 5°C).
- (2) cordierites₈₈ + olivine₈₈ + hercynite₈₈ from Chl₆₅Da₃₅ to Chl₄₇Da₅₃ over the temperature range 680–660°C (± 5°C).
- (3) cordierite₈₈ + olivine₈₈ + magnetite₈₈ somewhere in the region of Chl₄₇Da₅₃ to Chl₄₅Da₅₅ over the temperature range of approximately 660–655°C (± 5°C).
- (4) cordierite₈₈ + orthoamphibole₈₈ + magnetite₈₈ from Chl₄₅Da₅₅ to Chl₂₇Da₇₃ over the temperature range 665–625°C (± 5°C).
- (5) cordierite₈₈ + quartz + magnetite₈₈ from Chl₂₇Da₇₃ to Chl₀Da₁₀₀ over the temperature range 625–535°C (± 5°C).

Assemblage 3 (cordierite₈₈ + olivine₈₈ + magnetite₈₈) has not been well established by ex-

TABLE 7. Refractive Index Determinations of Synthetic Cordierite

Composition	Run No.	Assemblage	n_a	n_b
Mg cordierite	(1)			1.532
Chl ₉₀ Da ₁₀	161M	(i)	n.d.	1.537 ± 0.001
Chl ₇₅ Da ₂₅	164M	(i)	1.537 ± 0.001	n.d.
Chl ₆₀ Da ₄₀	155M	(ii)	1.540 ± 0.002	1.546 ± 0.001
Chl ₅₀ Da ₅₀	173M	(ii)	1.545 ± 0.001	1.550 ± 0.001
Chl ₄₀ Da ₆₀	150(B)M	(iv)	1.548 ± 0.002	n.d.
Chl ₂₀ Da ₈₀	171(B)M	(iv)	1.553 ± 0.002	n.d.
Fe cordierite	(1)			1.572

(1) from Hsu and Burnham (1969).

TABLE 8. Cell Dimensions of Synthetic Cordierite Coexisting with Olivine and Hercynite-Spinel

Bulk Composition	Run No.	a_o (Å)	b_o (Å)	c_o (Å)	V_o (Å) ³	N
Mg Cordierite	(1)	9.718 ± 0.004	17.056 ± 0.007	9.345 ± 0.003	1549.77 ± 0.71	13
Chl ₉₀ Da ₁₀	160M	9.764 ± 0.008	16.988 ± 0.019	9.365 ± 0.009	1553.30 ± 1.73	34
Chl ₈₀ Da ₂₀	148(C)F	9.771 ± 0.009	16.968 ± 0.012	9.376 ± 0.009	1554.55 ± 1.28	23
Chl ₇₀ Da ₃₀	147F	9.733 ± 0.012	17.049 ± 0.015	9.374 ± 0.013	1555.60 ± 2.14	18
Chl ₆₀ Da ₄₀	142F	9.727 ± 0.001	17.058 ± 0.019	9.396 ± 0.014	1559.10 ± 2.08	33
Chl ₅₀ Da ₅₀	173M	9.791 ± 0.010	17.062 ± 0.012	9.351 ± 0.011	1562.21 ± 1.50	23
Chl ₄₀ Da ₆₀	169(C)M	9.689 ± 0.012	16.941 ± 0.031	9.418 ± 0.010	1545.48 ± 2.49	9
Chl ₃₀ Da ₇₀	150(B)M	9.728 ± 0.019	17.164 ± 0.019	9.343 ± 0.016	1559.99 ± 3.68	9
Chl ₂₅ Da ₇₅	179(A)M (2)	9.692 ± 0.018	17.019 ± 0.047	9.359 ± 0.002	1543.38 ± 3.55	9
Chl ₂₀ Da ₈₀	171(B)M	9.757 ± 0.025	17.001 ± 0.057	9.385 ± 0.024	1557.82 ± 4.83	10
Fe Cordierite	(3)	9.824 ± 0.01	17.234 ± 0.01	9.298 ± 0.01	1572	

(1) Synthetic magnesium cordierite from Schreyer and Schairer (1961).

(2) Not a true equilibrium assemblage.

(3) Synthetic iron cordierite (Fe/Fe + Mg = 0.92) from Schreyer (1965).

perimental results, but inspection of compatible assemblages shows that it is required between the two adjacent fields. The single data point within this field (750°C) gave an ambiguous result after 2811 hours in repeated runs (*i.e.*, Co(+) + Hc-sp + Mt + Ol + Ged(-) + En(-)). Also, satisfactory reversals demonstrating the stability of assemblage 5 have not been achieved and the interpretation of our data for these iron-rich compositions has drawn on studies of daphnite by Turnock (1960) and by James *et al* (1974). The reaction curve between the assemblages 1 and 2 was not defined. The limits of assemblage 3 were not adequately defined and are probably not detectable within the limits of error of the experi-

ments; the width of this field, however, has been shown to be extremely narrow. The reaction between assemblages 3 and 4 was located close to 735°C (± 5°C) at the Chl₄₀Da₆₀ composition, while that between assemblages 4 and 5 has been demonstrated to lie above 625°C (± 5°C) at the Chl₂₅Da₇₅ composition, below 650°C (± 5°C) at the Chl₂₀Da₇₅, and below 650°C (± 5°C) at the Chl₂₀Da₈₀ composition.

TABLE 9. Electron Microprobe Analyses of Synthetic Cordierite

Run No.	173M	150(B)M	179(A)M	171(B)M
Bulk Composition	Chl ₅₀ Da ₅₀	Chl ₃₀ Da ₇₀	Chl ₂₅ Da ₇₅	Chl ₂₀ Da ₈₀
SiO ₂	46.7	47.9	50.0	48.9
Al ₂ O ₃	36.0	35.0	34.2	33.3
FeO	5.27	9.19	9.89	11.9
MgO	11.2	8.76	7.89	6.47
recalculated on the basis of 18 oxygen				
Si	4.713}6.000	4.833}6.008	4.980}6.000	4.889}6.000
Al	1.287}	1.168}	1.020}	1.111}
Al	3.000	2.996	3.001	2.898
Fe	0.445}2.14	0.775}2.09	0.824}2.01	1.018}2.000
Mg	1.699}	1.316}	1.185}	0.985}

The analyses averages for 7, 5, 3 and 4 grains in each of the four samples. Numerous points were analysed in each grain and the analyses are considered accurate to ± 3% of the amount present.

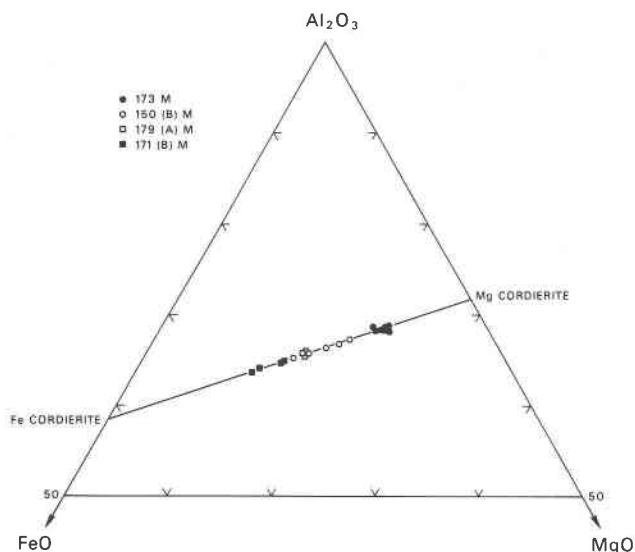


FIG. 5. Electron microprobe analyses of cordierite grains. Each point represents an average of numerous spot analyses within a single grain. Distribution of symbols indicates the compositional range of cordierites in a single experiment. (Figure in wt percent)

Metastable phases encountered include the 7Å chlorite polymorph and talc, both of which have been shown to disappear from a reaction product with increased duration of the experiment. Enstatite was identified as a product in several of the highest temperature experiments but a stable assemblage has not been defined that includes this phase. An unidentified 10Å phase has also been found occasionally associated with chlorite. Table 13 lists experimental data that define the curves shown in Figure 7. Some additional results from unreversed experiments are also shown in the figure and table.

James *et al* (1974) have shown quite clearly that orthoamphibole is not stable as a breakdown product of daphnite at a total water pressure of 2 kbar and at this pressure a reaction from cordierite + quartz + magnetite (assemblage 5) to almandine + quartz + magnetite should occur at approximately 810°C. The results of present study, however, suggest this reaction should occur in the region of 720°C at the NNO buffer for the daphnite composition. Ganguly (1972, Fig. 5) showed that the assemblage cordierite + magnetite + quartz may be related to the almandine bearing assemblage by a simple redox reaction. He has also pointed out (personal communication) that the equilibrium boundary for this reaction lies very close to the NNO buffer in the temperature interval 700°C to 800°C at 2 kbar. This may help show the relation between the two sets of results but does not explain why they differ. Greenwood (1963) has determined the upper stability limit of the orthoamphibole anthophyllite to be 770°C for a water pressure of 2 kbar. In the present set of experiments almandine was not encountered as a reaction product, and the position of the curve limiting the orthoamphibole field can only be inferred.

Balanced equations to represent the breakdown reactions of chlorite may be written as follows:

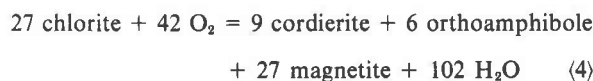
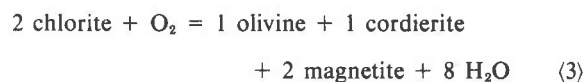
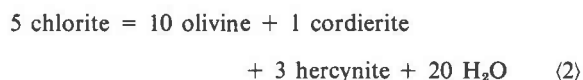
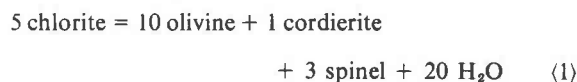
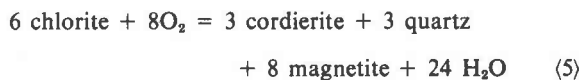


TABLE 10. Observed d Spacings for Orthoamphibole Coexisting with Cordierite and Magnetite*

Bulk Composition	Chl ₄₀ Da ₆₀	Chl ₃₀ Da ₇₀	Chl ₂₅ Da ₇₅	Chl ₂₀ Da ₈₀	
Run number	169(C)M	150(B)M	179(A)M	171(B)M	
hkl	d obs (Å)	d obs (Å)	d obs (Å)	d obs (Å)	I/I ₀
020	8.981	9.109	8.922	8.977	2
210	8.167	8.297		8.249	5
400	4.650			4.654	1
410	4.538	4.517	4.523	4.654	1
031				4.004	1
311			3.916		1
131		3.854			1
430		3.674			1
421	3.424	3.232	3.244	3.224	4
440					
521	2.882	2.899		2.895	2
251	2.830	2.826	2.818		2
630		2.750		2.754	2
112		2.592			1
102	2.586				2
270	2.469	2.469			1
271	2.232		2.223		1
561		2.132			1
181	2.044				1
661	1.994	1.995	1.994		1
712				1.871	1
113				1.758	1
392		1.541			1
543		1.500			1
2,10,2	1.460				1

* The error observed in each d obs. is $\pm 0.1^\circ 2\theta$ for Fe $K\alpha$ radiation.



Where cordierite compositions were determined by the electron microprobe, an accurate analysis of the compositions of the coexisting phases was possible since the composition of the experiment was unchanged and the iron component was treated as FeO. For reaction (4), a balanced breakdown reac-

TABLE 11. Calculated Orthoamphibole Compositions

Bulk composition	Chl ₃₀ Da ₇₀	Chl ₂₅ Da ₇₅	Chl ₂₀ Da ₈₀
Sample	150(B)M	179(A)M	171(B)M
SiO ₂	50.67	46.85	45.87
Al ₂ O ₃	12.89	13.91	14.00
MgO	25.51	20.02	15.76
FeO	10.94	19.23	24.36
Total	99.91	100.01	99.99
Si	6.37	6.03	6.17
Al	1.63	1.97	1.83
Al	0.28	0.14	0.39
Mg	4.78	3.84	3.16
Fe	1.15	2.07	2.74
Al/4	0.48	0.53	0.56
Fe/Fe + Mg	0.19	0.35	0.47

TABLE 12. Cell Parameters and Compositions of Synthetic Spinel

Bulk composition	Run number	a_o (Å)	V_o (Å) ³	N	Spinel composition (mol.% hercynite)
Chl ₁₀₀ Da ₀	(1)	8.075	526.54		0.00
Chl ₉₀ Da ₁₀	160M	8.088 ± 0.001	529.08 ± 0.26	7	17.5 ± 1.5
Chl ₈₀ Da ₂₀	148(C)F	8.100 ± 0.005	531.40 ± 1.50	5	34.0 ± 6.0
Chl ₇₀ Da ₃₀	147F	8.114 ± 0.002	534.27 ± 0.41	5	52.0 ± 2.5
Chl ₆₀ Da ₄₀	142F	8.153 ± 0.003	542.12 ± 0.62	5	88.8 ± 1.3
Chl ₅₀ Da ₅₀	173M	8.157 ± 0.003	542.78 ± 0.70	5	97.8 ± 1.3
Chl ₄₀ Da ₆₀	169(C)M	8.361 ± 0.006	584.42 ± 1.18	6	15.8 ± 2.8
Chl ₃₀ Da ₇₀	150(B)M	8.372 ± 0.004	586.86 ± 0.85	5	10.5 ± 2.5
Chl ₂₅ Da ₇₅	179(A)M	8.374 ± 0.002	587.27 ± 0.35	5	9.3 ± 1.2
Chl ₂₀ Da ₈₀	171(B)M	8.377 ± 0.005	587.99 ± 1.11	3	8.5 ± 2.0
Chl ₀ Da ₁₀₀	(2)	8.391	592.41		0.0

(1) Spinel from Warshaw and Keith (1954)

(2) Magnetite from Turnock and Eugster (1962)

The spinel coexisted with cordierite and olivine in lines 1 to 5 and with cordierite and orthorhombic amphibole for lines 6 to 9.

tion could not be written using the ideal gedrite end member formula and the formula $6(\text{Mg,FeO}) \cdot 1\frac{1}{2}\text{Al}_2\text{O}_3 \cdot 6\text{SiO}_2$ was found to be that which gave a satisfactory residual in the bulk composition calculations. The accumulated compositional data has been used to plot Fe/(Fe+Mg) ratios of coexisting

phases against that same ratio in the bulk composition (Fig. 8). This diagram shows the compositional variation for individual phases in the five chlorite breakdown assemblages as a function of Fe/Fe+Mg of the bulk composition. Olivine tends to reflect closely the Fe/Fe+Mg ratio of the bulk composition but spinel is enriched in iron. Cordierite and amphibole are enriched in Mg but the range in cordierite composition noted earlier (Fig. 5) probably applies to all phases. The internal consistency of the data suggest a general approach to equilibrium in the experimental results.

Petrologic Application

The compositions of certain ultramafic rocks closely approach compositions that have been investigated experimentally in the system $\text{MgO-FeO-Al}_2\text{O}_3\text{-SiO}_2\text{-H}_2\text{O}$. Accounts of ultramafic rocks that have undergone low-pressure, high-temperature contact metamorphism are relatively few. One of the best documented occurrences is from California where granodioritic stocks, related to Sierra Nevada batholith, intrude a regionally metamorphosed sequence that contains highly serpentized dunites.

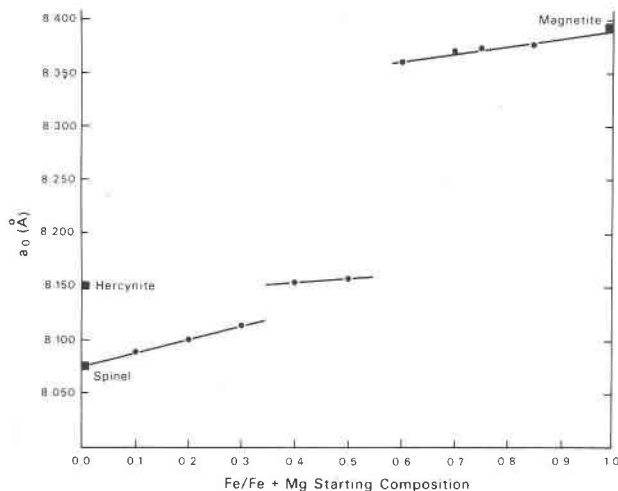


FIG. 6. Plot of estimated spinel compositions from the data of Table 12.

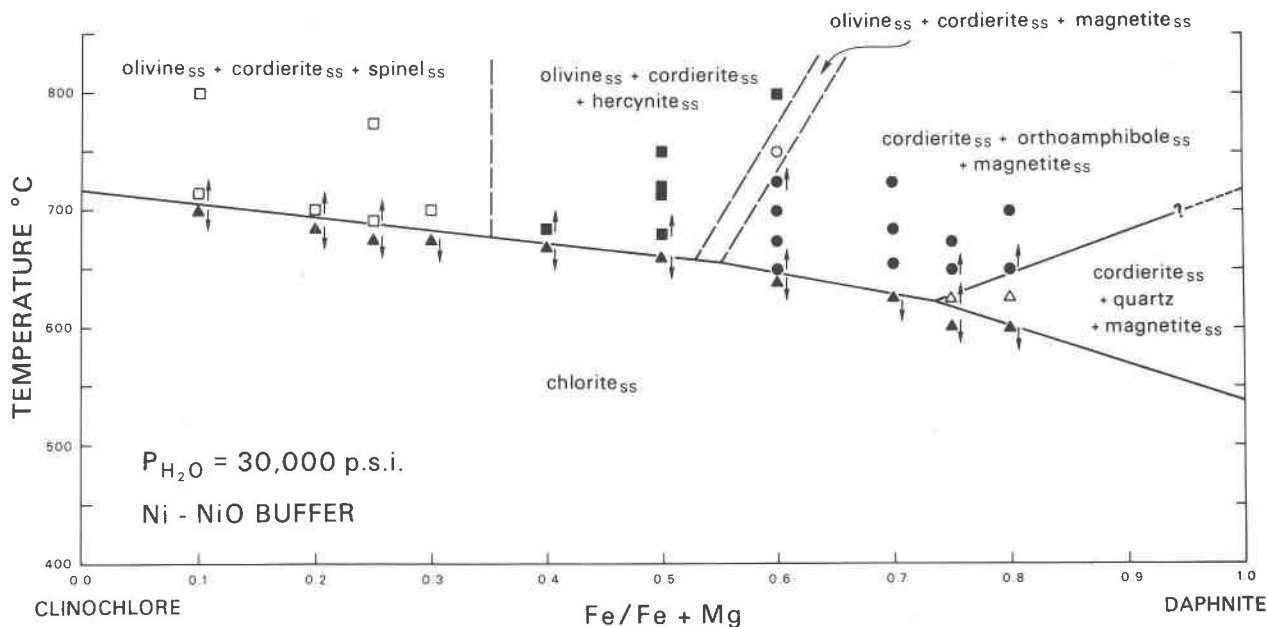


FIG. 7. T - X projection at 2.07 kbar P_{H_2O} of experimental results for the join clinocllore- $Mg_5Al_2Si_3O_{10}(OH)_8$ -daphnite- $Fe_5Al_2Si_3O_{10}(OH)_8$ under the NNO buffer. Arrows pointing to higher temperatures indicate the particular result was obtained with the lower temperature assemblage as starting material, and vice versa for arrows pointing to lower temperatures (*i.e.*, indicators of reaction reversals).

Durrell (1940) described the following assemblages from contact metamorphosed ultramafic rocks:

1. clinocllore + talc + actinolite—outer zone of aureole
2. forsterite + clinocllore + tremolite + talc—inner zone of aureole
3. forsterite + clinocllore + enstatite + spinel

All phases were considered to be non-primary; however, much of the chlorite and possibly talc were thought to be secondary retrograde minerals. Using the results of Yoder's (1952) experimental work (clinocllore = forsterite + cordierite + spinel + vapor), Fyfe, Turner, and Verhoogen (1958) considered the occurrence of the orthopyroxene to be perhaps due to the addition of FeO to this system, or that it may indicate a water pressure higher than those of the experiments. The subsequent study by Fawcett and Yoder (1966) showed that forsterite + enstatite + spinel is the stable breakdown assemblage of clinocllore above 3.25 kbar water pressure at 765°C.

The present study at 2.07 kbar water pressure has shown that the addition of FeO does not permit orthopyroxene as a stable phase for the clinocllore-daphnite compositions. Bulk compositions of assemblages described by Durrell are not known but they clearly differ, in varying degrees, from composi-

tions investigated experimentally. In the critical assemblage (number 3, above), the occurrence of enstatite + spinel indicates that the contact metamorphic assemblage equilibrated at pressures greater than about 3.25 kbar and temperatures above 770°C, if $P_{total} = P_{H_2O}$ (see Fig. 1). In some cases the reported assemblages are quite calcium rich and the effect of this component is unknown. Springer (1971) has described contact metamorphic assemblages, from western Sierra Nevada, derived from ultramafic rocks composed largely of serpentine minerals with minor chlorite, talc, carbonate minerals, and altered chromite. Outward from the igneous contact the following mineral assemblages of the pyroxene hornfels facies were observed: orthopyroxene-olivine-aluminous spinel, anthophyllite-olivine-chlorite, and talc-olivine-chlorite. The ubiquitous presence of a calcic amphibole in each of these assemblages, however, does not allow direct correlation with the system investigated. Springer considered the physical conditions of metamorphism to be near 750°C and 3 kbar water pressure at the igneous contact, which is consistent with evidence from experimental studies.

Spence (1969) has ascribed the origin of cordierite-anthophyllite bearing rocks found in alteration pipes below some of the base metal deposits of the Rouyn-Noranda area to isochemical thermal metamorphism of rocks composed almost entirely of

TABLE 13. Results of Experiments with Compositions on the Join Clinochlore-Daphnite at 2.07 kbar P_{H_2O} and at Oxygen Fugacities of the NNO Buffer

Run No.	Temperatures in degrees C	Duration in hours	Starting Material	Products
Composition: Clinochlore ₉₀ Daphnite ₁₀ (mix 6)				
146F	800	49	oxide mix	Co + Ged + Hc-sp + Ol
146(A)F	700	428	Co + Ged + Hc-sp + Ol	Co + Ged(-) + Hc-sp + Ol
145(B)F	700	648	product of 146(A)F	Hc-sp + Ol
146(C)F	700	4896	product of 146(B)F	Chl
160M	717.7 ± 1.8 n = 19	1034	product of 146(C)F	Co + Hc-sp + Ol
Composition: Clinochlore ₈₀ Daphnite ₂₀ (mix 7)				
148F	700	526	oxide mix	Chl + Hc-sp + Ol + Tc
148(B)F	700	946	product of 148F	Chl(-) + Co(+) + Hc + Ol + Tc(-)
148(C)F	700	2712	product of 148(B)F	Co + Hc-sp + Ol
159M	685.3 ± 2.1 n = 16	1041	product of 148(C)F	Chl(+) + Co + Hc-sp(-) + Ol
Composition: Clinochlore ₇₅ Daphnite ₂₅ (mix 5)				
133(A)F	775	166	oxide mix	En + Hc-sp + Ol
163M	691 ± 1.7 n = 12	592	Chl	Chl(-) + Co(+) + Hc-sp + Ol(+)
164M	675.6 ± 2.6 n = 11	671	Co + Hc-sp + Mt(?) + Ol + Tc	Chl(+) + Co(-) + Hc-sp(-) + Ol(-)
Composition: Clinochlore ₇₀ Daphnite ₃₀ (mix 8)				
147(B)F	675	785	Co + Hc-sp + Ol + Tc	Co + Ged(+)? + Hc-sp + Ol
165M	673.4 ± 1.3 n = 14	926	product of 147(B)F	Chl(+) + Co(-) + Ged?
147F	700	480	oxide mix	Co + Hc-sp + Ol + Tc
Composition: Clinochlore ₆₀ Daphnite ₄₀ (mix 9)				
154M	670.8 ± 3.2 n = 37	1608	Co + Hc-sp + Ol	Chl(+) + Co(-) + Ged(+)? + Hc-sp + Ol(-)
155	686.7 ± 1.6	1584	Chl + Co + Ged(?)	Co(+) + Hc-sp(+) + Ol(+) + Tc(-)?

TABLE 13. Continued

Run No.	Temperatures in degrees C	Duration in hours	Starting Material	Products
Composition: Clinocllore ₅₀ Daphnite ₅₀ (mix 3)				
121J	660	514	Co + Hc-sp + Ol	Chl(+) + Co + Hc-Sp(-) + Ol(-)
183J	680	360	Chl + Ol + Tc	Chl + Co(+) + Hc-sp(+) + Ol(+)
68J	715	720	oxide mix	Co + Hc-sp + Ol
120J	720	514	Chl + Co + Hc-sp + Ol + Tc	Co(+) + Hc-sp(+) + Ol(+)
173M	750.0 ± 0.6 n = 14	1408	oxide mix	Co + Hc-sp + Ol
Composition: Clinocllore ₄₀ Daphnite ₆₀ (mix 10)				
152M	652.4 ± 3.9 n = 38	1608	Chl + Co + Ged + Mt	Chl(-) + Co(+) + Ged(+) + Mt
153M	641.5 ± 3.5 n = 36	1584	Co + Ged + Hc-sp + Ol + Tc	Chl(+) + Co + Ged + Hc-sp + Mt(+)
174(A)M	676.2 ± 1.2 n = 6	720	Chl + Co + Ged + Hc-sp + Mt + Tc	Chl(-) + Co + Ged(+) + Hc-sp(-) + Mt
169(A)M	703.0 ± 1.4 n = 3	588	Co + Ged + Hc-sp + Mt + Ol	No change
169(B)M	726.4 ± 1.1 n = 7	554	Co + Ged + Hc-sp + Mt + Ol	Co(+) + Ged(+) + Hc-sp(-) + Mt(+)
168M	750.5 ± 0.9 n = 15	1070	oxide mix	En + Ged + Hc-sp + Mt + Ol
168(A)M	751.5 ± 0.7 n = 13	720	product 168M	Co + En(-) + Ged + Hc-sp + Mt + Ol
168(B)M	749.7 ± 2.8 n = 20	1021	product 168(A)M	Co(+) + En + Ged(-) + Hc-sp + Mt + Ol
167M	797.7 ± 2.1 n = 3	101	oxide mix	En + Ged + Hc-sp + Ol
Composition: Clinocllore ₃₀ Daphnite ₇₀ (mix 11)				
149	623.8 ± 2.2 n = 43	1752	oxide mix	Co + Ged + Hc-sp + Mt + Ol + Tc
149(A)M	625.0 ± 3.5 n = 7	552	product of 149M	Chl(+) + Co + Ged(+) + Hc-sp(-)
149(B)M	624.2 ± 2.1 n = 10	781	product of 149(A)M	Chl(+) + Co + Ged + Mt
151M	657.2 ± 1.4 n = 41	1728	oxide mix	Co + Ged + Hc-sp + Mt
150(B)M	686.5 ± 1.0 n = 4	728	Co + Ged + Hc-sp + Mt + Ol(-)	Co(+) + Ged + Mt(+)
170M	725.5 ± 2.7 n = 26	1980	oxide mix	Co + Ged + Hc-sp + Mt

TABLE 13, Continued

Run No.	Temperatures in degrees C	Duration in hours	Starting Material	Products
Composition: Clinocllore ₂₅ Daphnite ₇₅ (mix 4)				
85F	625	2808	oxide mix	Chl + Mt + Ol + Qtz + Tc
101F	600	3168	oxide mix	Hc-sp + Mt + Ol + Qtz + Tc
175M	624.4 ± 3.1 n = 16	1888	product of 85F	Chl + Co(+) + Mt + Ol? + Qtz
175(A)M	624.4 ± 0.9 n = 15	1008	product of 175M	Chl(-) + Co(+) + Mt(+) + Ol + Qtz
178M	602.3 ± 7.2 n = 21	1575	product of 101F	Chl(+) + Co + Mt + Qtz
179M	651.6 ± 1.6 n = 13	1320	oxide mix	Chl + Co + Ged? + Mt + Tc
179(A)M	649.3 ± 3.3 n = 22	1021	product of 179M	Co + Ged(+) + Mt + Tc(-) + ?
177M	675.2 ± 3.1 n = 19	1621	oxide mix	Ged + Hc-sp + Mt + Ol + Qtz
Composition Clinocllore ₂₀ Daphnite ₈₀ (mix 12)				
182(A)M	598.8 ± 0.9 n = 10	781	Chl + Mt + Qtz	Chl(+) + Qtz(-) + Mt(-)
181M	625.5 ± 1.9 n = 20	1023	oxide mix	Chl + Co + Hc-sp + Mt + Ol + Qtz
172M	651.4 ± 4.4 n = 23	1121	oxide mix	Chl + Co + Ged + Hc-sp + Mt + Qtz
172(A)M	652.0 ± 3.4 n = 7	720	product of 172M	Chl(-) + Co(+) + Ged(+) + Hc-sp(-)
172(B)M	650.3 ± 1.4 n = 19	1023	product of 172(A)M	Co(+) + Ged(+) + Mt(+)
171(B)M	698.8 ± 1.0 n = 18	1023	Co + Ged + Mt + Qtz	Co + Ged + Mt

Temperatures on critical experiments are reported as the mean of n measurements ± 2 standard deviations.

chlorite. The primary siliceous volcanic rocks were hydrothermally altered to produce a chlorite-rich rock. Isochemical metamorphism converted the chlorite to the present cordierite-anthophyllite-ripidolite-magnetite assemblage. Quartz is present in the more siliceous varieties, and later alteration has caused the formation of a second chlorite and pinitic alteration of cordierite. This contact metamorphic assemblage may be compared directly with assemblage 4 determined from the present study. A whole rock analysis of the hydrothermal chlorite rock supplied by Spence shows this to lie within the investigated system and to have a bulk composition

with an Fe/Mg ratio close to that of the Chl₆₀Da₄₀ composition, but to be about 10 percent richer in Al₂O₃ when recalculated to the AFM end members. This may indicate a larger range for the cordierite-orthoamphibole-magnetite stability field for intermediate magnesian-iron chlorites with a higher alumina content than the clinocllore-daphnite solid solution series. Compositional data for the natural assemblage described above is not available; the names anthophyllite and ripidolite were derived from thin section studies and must be considered applied loosely. If it is assumed that at the time of recrystallization total water pressure was 2 kbar and f_{O_2} is

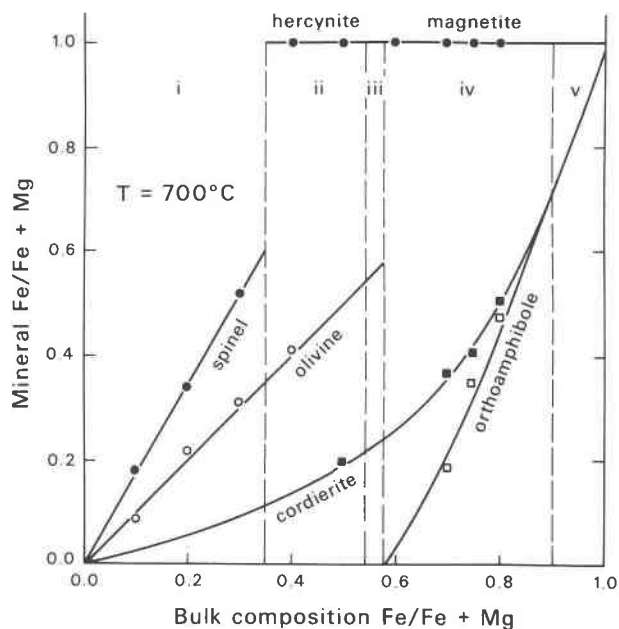


FIG. 8. Fe/Fe+Mg ratios for individual phases in the five chlorite breakdown assemblages as a function of Fe/Fe+Mg in the bulk composition. Numbers i to v are the various chlorite breakdown assemblages as in Figure 7 and all data are for experiments at 700°C and 2.07 kbar P_{H_2O} under the NNO buffer.

similar to that of the experiments, a temperature range of 620°C to 660°C is considered a reasonable estimate of the metamorphic temperatures involved in the formation of these cordierite-anthophyllite rocks.

Acknowledgments

This paper is based on the Master of Sciences thesis of the senior author with additional experimental work by both junior authors. Mr. I. Davies was particularly helpful in dealing with equipment problems. G. M. Anderson, R. A. F. Grieve, and G. W. Bird discussed many aspects of the work with us, and J. Ganguly provided a helpful review of the manuscript. J. C. Rucklidge provided instruction in use of the electron microprobe that is supported by his grants from the National Research Council of Canada. The experimental work was supported by an operating grant from the National Research Council of Canada to the second author.

References

- APPLEMAN, D. E., S. D. HANDWERKER, AND H. T. EVANS (1963) The least squares refinement of crystal unit cell with powder diffraction data by an automatic computer indexing method (abstr.). *Program Annu. Meet. Am. Crystallogr. Assoc.*
- BAILEY, S. W. (1972) Determination of chlorite compositions by X-ray spacings and intensities. *Clays Clay Minerals*, **20**, 381-388.
- CHERNOSKY, J. V. (1974) The upper stability of clinocllore at low pressure and the free energy of formation of Mg-cordierite. *Am. Mineral.* **59**, 496-507.
- DEER, W. A., R. A. HOWIE, AND J. ZUSSMAN (1962) *Rock Forming Minerals*, Volume 1, Longmans.
- DURRELL, C. (1940) Metamorphism in the southern Sierra Nevada northeast of Visalia, California. *Univ. Calif. Publ., Dep. Geol. Sci. Publ.*, **25**, 1-118.
- EUGSTER, H. P. (1957) Heterogeneous reactions involving oxidation and reduction at high pressures and temperatures. *J. Chem. Phys.* **26**, 1760.
- (1959) Reduction and oxidation in metamorphism. In: *Researches in Geochemistry*. John Wiley and Sons, Inc., N. Y., p. 397-426.
- FAWCETT, J. J., AND H. S. YODER (1966) Phase relationships of chlorites in the system MgO-Al₂O₃-SiO₂-H₂O. *Am. Mineral.* **51**, 353-380.
- FISHER, G. W. (1966) Fe-Mg olivine solid solutions. *Carnegie Inst. Wash. Year Book*, **65**, 209-217.
- FYFE, W. S., F. J. TURNER, AND J. VERHOOGEN (1958) Metamorphic reactions and metamorphic facies. *Geol. Soc. Am. Mem.* **73**.
- GANGULY, J. (1972) Staurolite stability and related parageneses: theory, experiments and applications. *J. Petrol.* **13**, 335-365.
- GREENWOOD, H. J. (1963) The synthesis and stability of anthophyllite. *J. Petrol.* **4**, 317-351.
- HEY, M. H. (1954) A new review of the chlorites. *Mineral. Mag.* **30**, 272-292.
- HSU, L. C., AND C. W. BURNHAM (1969) Phase relationships in the system Fe₃Al₂Si₃O₁₂-Mg₃Al₂Si₃O₁₂-H₂O at 2.0 kilobars. *Bull. Geol. Soc. Am.* **80**, 2393-2408.
- JAMES, R. S., A. C. TURNOCK, AND J. J. FAWCETT (1974) The stability of iron chlorite below 10 kbar. Unpublished manuscript.
- NELSON, B. W., AND R. ROY (1958) Synthesis of the chlorites and their structural and chemical constitution. *Am. Mineral.* **43**, 707-725.
- PHILLIPS, F. G. (1930) An association of anthophyllite and enstatite. *Geol. Mag.* **67**, 513-516.
- PUTNAM, G. W., AND J. T. ALFORS (1969) Geochemistry and petrology of the Rocky Hill stock, Tulare county, California. *Geol. Soc. Am. Spec. Pap.* **120**.
- RUCKLIDGE, J. C. (1969) Specifications of a computer program for processing electron microprobe analytical data—EMPADR. Department of Geology, University of Toronto.
- , F. G. F. GIBB, J. J. FAWCETT, AND E. L. GASPARRINI (1970) Rapid rock analysis by electron probe. *Geochim. Cosmochim. Acta*, **34**, 243-247.
- SCHREYER, W. (1965) Zur Stabilität des Ferrocordierits. *Beitr. Mineral. Petrogr.* **11**, 297-322.
- , AND J. F. SCHAIRER (1961) Compositions and structural states of anhydrous Mg-cordierites: A reinvestigation of the central part of the system MgO-Al₂O₃-SiO₂. *J. Petrol.* **2**, 324-406.
- SEGNIT, R. E. (1963) Synthesis of clinocllore at high pressures. *Am. Mineral.* **48**, 1080-1089.
- SPENCE, A. (1969) Genese des roches a cordierite-anthophyllite des gisements cupro-zinciferes de la region de Rouyn-Noranda, Quebec, Canada. *Can. J. Earth Sci.* **6**, 1339-1345.
- SPRINGER, R. K. (1971) Contact metamorphosed ultramafic rocks in the western Sierra Nevada foothills, California (abstr.). *Geol. Soc. Am.* **3(5)**, 349-350.
- TURNOCK, A. C. (1960) The stability of iron chlorites. *Carnegie Inst. Wash. Year Book*, **59**, 98-103.
- TURNOCK, A. C., AND H. P. EUGSTER (1958) Magnetite-hercynite relations. *Carnegie Inst. Wash. Year Book*, **57**, 209.

- , AND ——— (1962) Fe-Al oxides: Phase relationships below 1000°C. *J. Petrol.* **3**, 533-569.
- TUTTLE, O. F. (1949) Two pressure vessels for silicate-water studies. *Bull. Geol. Soc. Am.* **60**, 1727-1729.
- WARSHAW, I., AND M. L. KEITH (1954) Solid solution and chromium loss in part of the system MgO-Al₂O₃-Cr₂O₃-SiO₂. *J. Am. Ceram. Soc.* **37**, 161.
- YODER, H. S. (1952) The MgO-Al₂O₃-SiO₂-H₂O system and the related metamorphic facies. *Am. J. Sci., Bowen vol.*, 569-627.
- , AND T. G. SAHAMA (1957) Olivine X-ray determinative curve. *Am. Mineral.* **42**, 475-491.
- ZEN, E-AN (1972) Gibbs free energy, enthalpy, and entropy of ten rock forming minerals: calculation, discrepancies, implications. *Am. Mineral.* **57**, 524-553.

*Manuscript received, March 19, 1975; accepted
for publication, July 10, 1975.*